Measurement of the charge distribution deposited on a target surface by an annular plasma synthetic jet actuator: Influence of humidity and electric field

Measurement of the charge distribution deposited on a target surface by an annular plasma synthetic jet actuator: influence of humidity and electric field.

A.C. Ricchiuto[1], C.A. Borghi[1], A. Cristofolini[1], and G. Neretti[1]*

1 Department of Electrical, Electronic and Information Engineering, University of Bologna, Italy

E-mail: annachiara.ricchiut2@unibo.it

Abstract

In this paper, an investigation on an annular Plasma Synthetic Jet Actuator (PSJA) utilizing a Surface Dielectric Barrier Discharge (SDBD) is reported. The work is focused at an investigation of the electric charges transported by the jet produced by the actuator and deposited on a target. Particularly, an assessment of the various factors that may affect the charge deposit process has been carried out. Experiments have been performed in a controlled environment with different electric configurations. This allowed to evaluate how the humidity rate affects and the dynamics of the electric charge build-up process. It was observed that humidity rate weakly affects the charge deposition, being the most notable effect an increase of the deposition time for higher humidity rate. Moreover, the performances of two different power supply systems, working at different voltage and frequency conditions, were compared. The two supplies have been set up do feed the actuator with the same power, in order to assess which voltage-frequency condition is more efficient at depositing electric charge on the target. It was observed that a higher applied electric field produces higher charge deposition rates.

Keywords: non-thermal plasma, dielectric barrier discharge, electro hydro dynamics, plasma actuator, charge distribution, relative humidity, electric field

1. Introduction

Non-thermal atmospheric pressure plasma treatments have been intensively investigated in the last decades. The ability of these treatments to inactivate several species of pathogens has been shown [1] [2] [3] [4] [5] [6] [7]. Dielectric Barrier Discharges (DBDs) are often used as non-thermal plasma sources. They generate homogeneously distributed non-thermal cold plasmas at atmospheric pressure and a gas temperature near the room temperature above the SDBD actuator surface [4]. The most relevant advantages of DBD plasma treatments are their low operational cost, due to room temperature and pressure operation, the absence of residual and toxic emissions, the scalability, and the possibility to utilize air as plasma gas and carrier gas. The use of atmospheric pressure air is one of the most important aspect to be taken into account when considering the applicability of this technology in sterilization treatments.

Direct and indirect plasma treatments have been investigated in the last years [1], [9]. Indirect treatments are generally used to treat irregular or large surfaces and with complex geometries. In this study, the use of Electro-Hydro-Dynamic (EHD) interaction [10] [11] [12] to obtain a flow of air containing charged particles and active species by means of a Surface DBD plasma for the indirect treatment is investigated. The EHD interaction induced by a SDBD is mainly due to

the acceleration of the ions, obtained by the electrostatic effect on the plasma sheath. The acceleration of the gas inside the boundary layer is due to the momentum gained by the charged particles accelerated by the electric field, which in turn drag the neutral particles with them [13]-[16]. The induced wind will transport neutral particles, active species, and free charged particles, too. These charges are partially deposited on the dielectric surface of the SDBD actuator and can strongly modify discharge regime and EHD effect [17]-[21].

Plasma Synthetic Jet Actuators (PSJAs) generate a flow containing charged particles perpendicular to the surface of the SDBD actuator where the plasma discharge is ignited, [22] [23]. The PSJA indirect treatment exposes the skin of pathogens or cells to react with oxygen, nitrogen species (RNOS), and with a significant amount of charged particles [24] [25]. These species are transported by the ionic flow coming from the actuator where the plasma is produced and flow toward the target surface to be treated. The plasma jet propagates for several centimetres at a velocity of some metres per second. It generates an anisotropic treatment, enhancing the species transport rate and increasing the treatment efficacy [12], [26].

In a recent work, our research group used PSJA to treat *Candida Guillermondii* through the indirect method. In it, the investigation about the role of charged particles in the inactivation process was described [3]. Charged particles transported by the induced jet led to a remarkable reduction of *Candida* pathogens for long treatment times. All tests were performed in atmospheric pressure air and non-controlled conditions. Recently, Abdelaziz et al. investigated the role of humidity in the naphthalene decomposition and its influence on the discharge mechanism [27]. The results pointed out the importance of humidity in SDBD plasma treatments.

The present paper aims to investigate the influence of humidity on the plasma discharge and on the charged particles transported by the induced flow in the neighbourhood of a PSJA and indirectly deposited on a target placed 2 cm far from the SDBD actuator. This distance guarantees to be far enough from the plasma and that the treatment, which can be obtained, is indirect. Moreover, the influence of the voltage and frequency of the power supply on the quantity of the charges deposited on the target have been studied. This has been done by varying the supply working conditions while keeping unchanged the average power supplied to the discharge and the EHD effect. The results will be utilized to improve charged particles production and delivery, and to evaluate the possibility to utilize these actuators for decontamination purposes in non-controlled ambient conditions.

2. Materials and methods

Experiments were carried out by using the annular PSJA characterized by the octagonal geometry investigated in [26]. The annular PSJA utilizes a 2 mm thick PVC as dielectric material, and copper as exposed and buried electrodes **Figure 1**. The annular electrode has an octagonal geometry. Each side of the octagon has an inner length of 12 mm, a width of 5 mm and a thickness of 35 μm, **Figure 1**, the left-hand. The annular electrode is placed on a 2 mm thick dielectric slab. Under the dielectric the second electrode is placed, **Figure 1**, the right-hand. It is an octagonal slab of a side of 12 mm and a thickness of 35 μm.

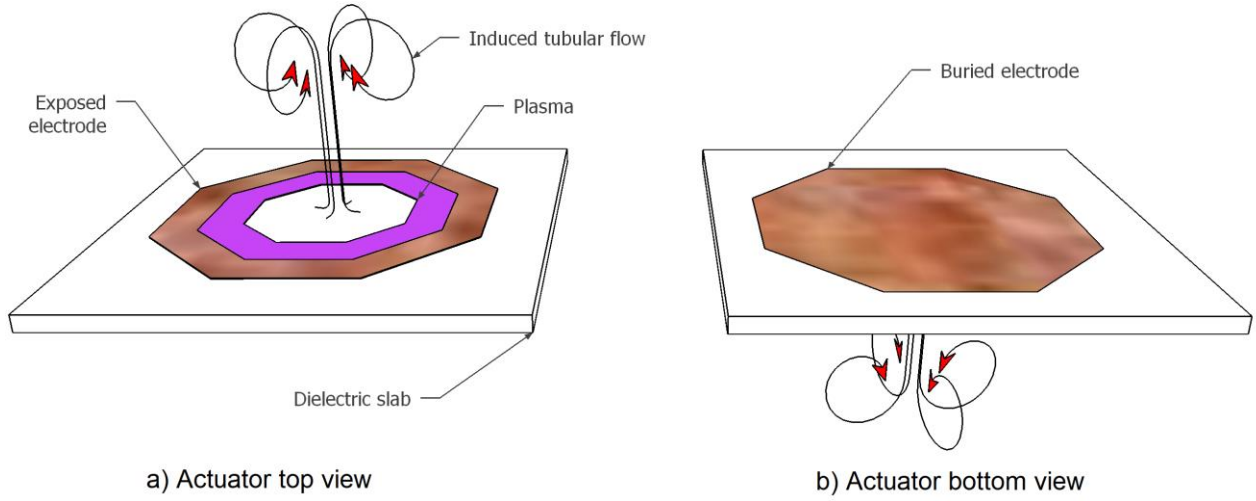

Figure 1 Octagonal PSJA sketch.

The octagonal PSJA is obtained by eight jets tangential to the actuator surface and colliding when approaching the centre of the octagonal exposed electrode. After their merging, a normal tubular flow is generated perpendicularly to the surface. This jet transports both reactive species and charged particles toward the target surface. The jet propagates for several centimetres at a velocity of some metres per second [26] [28].

Two power supplies with different electrical parameters and the same plasma average power together with the same EHD effect have been used to ignite the discharge. A first series of experiments have been carried out by using a sinusoidal supply system constituted by a push–pull high voltage transformer controlled by an Arduino, as described in reference [29]. This power source will be referred to as Power Supply 1. It allows to change both voltage and frequency in the range 0–20 kVp and 15–50 kHz respectively. It can ignite the plasma with an arbitrary duty cycle. For the actuator considered in this work, a sinusoidal voltage of 6 kV peak and a frequency of 31 kHz have been used. With these high voltage and frequency discharge power supply has been of 10 W.

In order to investigate the influence of the magnitude of the electric field on charge production and transport, a second supply system has been utilized. The system, hereafter referred to as Power Supply 2, is constituted by a signal generator, a power amplifier, and a step-up transformer, as described in Ref. [11]. The signal generator (HP-Agilent 33120-A) produces a low-voltage AC signal with a frequency of 4.2 kHz that is delivered to the amplifier (Elgar Model 3001 AC). It allows to change the frequency in the range of 4 – 15 kHz. A high voltage ferrite transformer is then used to reach the desired output high voltage. The power supply has been set at a 12 kV peak sinusoidal output voltage, at an average power of 10 W, which is the same value used in tests carried out with the Power Supply 1. As a consequence of this, the EHD effect is the same [30].

In this work, five humidity rate (HR) values have been investigated: 5 %, 25 %, 45 %, 60 % and 80 %. As far as the results obtained at 25 %, 45 % and 60 % humidity, rates were the same (within the experimental errors) only data acquired for the 5 %, 45 % and 80 % tests will be reported and discussed. The rates of 5 % and 80 % are at extreme and opposite conditions and the rate of 45 % is the intermediate and usual ambient condition (usually between 40% and 60%).

In order to control the temperature and the humidity of the air, a PVC cubic airtight box with a 15 cm long edge, has been used. The box is provided with a glass wall allowing a visual inspection of the test region. A Plexiglass movable tray, placed at the bottom of the box, has been used to measure charged particles. A copper tape has been set below the tray

and has been grounded allowing stable and reliable measurements of the induced potential (**Figure 2**). The movable tray and the box dimensions have been chosen to have a small control volume and to guarantee quick humidity conditions before each test. In the box, the air temperature was maintained at 25 °C. Synthetic air was used. Humidity and temperature have been measured by using two sensors controlled by an Arduino UNO microcontroller. In order to avoid the electromagnetic noise produced by the discharge, the sensors were shielded by using a metallic grounded wire mesh. The humidity level was varied by flowing a portion of the air through a bubbling bottle filled with room temperature Demi water. The dry/damp air flow rate was controlled by a mass flow rate controller F-201CV with a flow rate of 6 l/min.

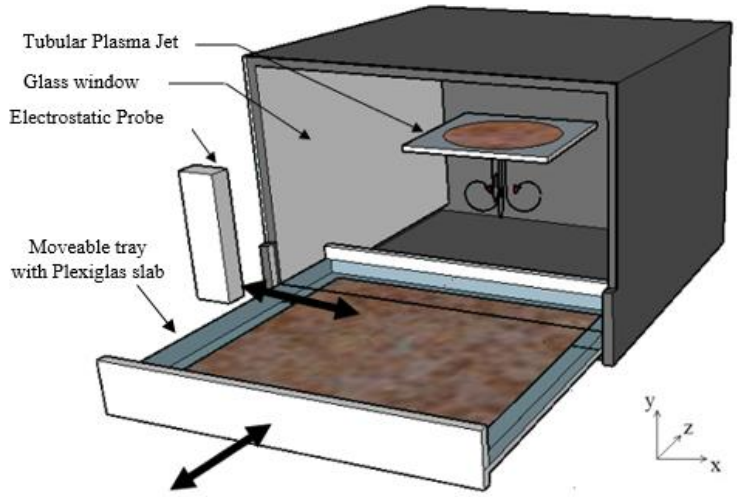

Figure 2 PVC cubic airtight box, electrostatic probe and PSJA position in the experimental set-up.

The overall schematic of the experimental set-up used in the present study is shown in **Figure 3**. During an experiment, the PSJA is placed in the box, over the tray, with its surface parallel to it at a distance of 20 mm (**Figure 3**). This is a typical distance for indirect treatments. The discharge is ignited for a given time interval. While the PSJA is active, a jet is formed in the negative y direction (x, y, and z directions are indicated in **Figure 3**), and electric charges are transported and deposited on the tray. After switching off the discharge, the movable tray is extracted and a scan in the x direction of the surface potential induced by the charge build-up is carried out. A 341B 20 kV TREK electrostatic voltmeter was utilized for this purpose. This instrument utilizes a field-nulling electrostatic voltage probe to measure the electric potential produced by the deposited charge without the need of an electric contact. The electrostatic voltage probe has been moved by means of an automated handler with a resolution of 0.1 mm.

The average power delivered to the discharge has been evaluated by using Lissajous figures [31]. The high voltage applied to the electrodes has been measured by means of a Tektronix P6015 capacitively compensated high voltage probe with a bandwidth up to 75 MHz. The voltage across the measuring capacitor Cm of 1 nF (Figure 3), used to evaluate the charge flowing within the discharge, has been detected by a Yokogawa low voltage probe with a 75 MHz bandwidth. In the figure, the exposed electrode is grounded and the buried one connected to the high voltage terminal. During the tests, the reverse configuration with the exposed electrode connected to the high voltage terminal and the buried one connected to the ground reference potential, has been utilized too. Both signals have been acquired with a Yokogawa DL1740 4-

channel, 500 MHz bandwidth, 1 GS s−1 oscilloscope. Charge distribution has been evaluated by means of the surface potential measurements and using the numerical approach described in [18].

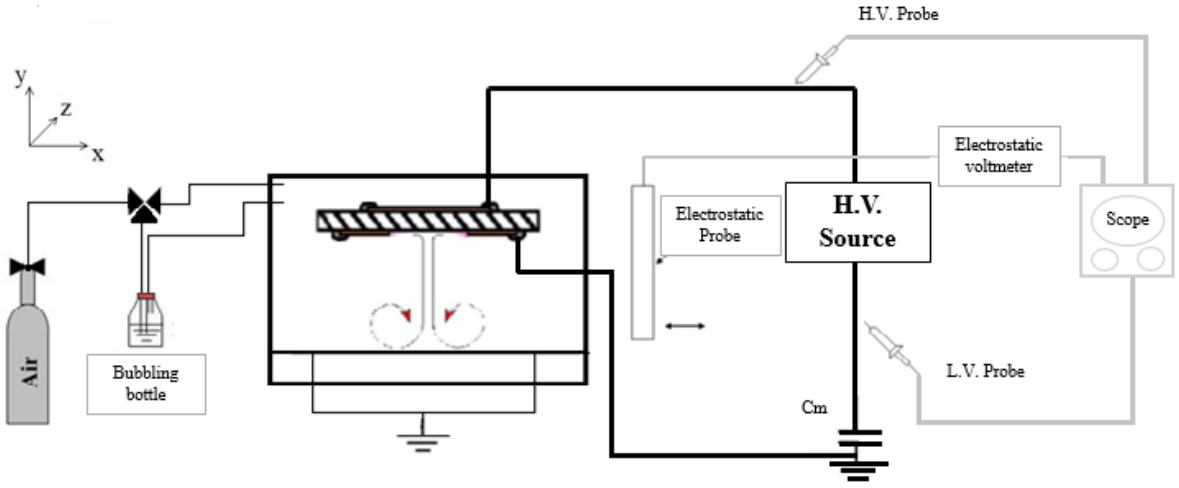

Figure 3 Experimental set-up schematic.

The experimental procedure has been performed through the following steps.

1. The box is closed, the humidity is set to the selected value by using the bubbling bottle and the mass flow controller.
2. The mass flow controller is switched off and the discharge is switched on for the defined time interval.
3. The discharge is switched off, the moveable tray is opened, the electrostatic probe is moved over the Plexiglass surface (along the x direction) in the region where the induced jet impinges the surface, and the induced potential signal is detected. The time between the two operations is only the time needed to open the movable tray, only few seconds.
4. The Plexiglass surface is wiped by using a wet cloth and then heated up for 10 s with a hot air gun to eliminate possible traces of humidity.
5. The electrostatic probe is moved back on the Plexiglass surface to make sure that a zero-voltage signal is present. When the zero-voltage condition is not achieved, steps 3 and 4 are repeated.
6. The movable tray is closed, and the set-up is ready for another test.

Steps 1 to 6 have been repeated for discharge ignition time intervals of 50 ms up to 20 s, for all humidity rates considered, with the actuator exposed electrode either connected to the high voltage terminal or grounded, and by supplying the discharge with the two power supplies. For each condition, five measurements have been done, reaching a standard deviation within 7 %.

3. Results and discussion

A first series of experiments has been done to evaluate how humidity conditions affect the recombination rate or the migration of the charged species deposited on the Plexiglass plate. After the discharge has been operated for the required time interval, the tray has been opened, and the charged particle distribution has been measured by means of the electrostatic probe. The electrostatic probe measurement has been repeated after 10 minutes, during which the tray has been kept closed in a controlled humidity environment. The results of the two measurements have been compared to estimate charge recombination/migration rate. This procedure has been repeated for the above mentioned humidity rates. For all the tested humidity rates, the measured charged particles distribution has not shown significant variations in the 10 minutes considered. This test has shown that, in the experimental conditions investigated, the charged particle recombination and/or migration from the Plexiglass surface is slightly dependant on the humidity rate. Moreover, it has been observed that the charged particles remain attached to the Plexiglass slab for very long-time intervals (in the order of tens of minutes). This guarantees the reliability of the measurement set-up used for this investigation.

The average power supplying the discharge has been evaluated by using the Lissajous figure method [31]. For all the humidity conditions investigated, the same value of the average power, within a standard deviation error of the 5%, has been obtained. The following expression of the power has been utilized:

$$P = {}^{1}/_{T} \oint v_{out}(t)\, dq_m$$

The integral is the expression of the energy delivered to the discharge in a voltage period T, corresponding to the area inside the voltage-charge cycle of the Lissajous graph. For all tests, the average power of 10 W, supplying the discharge, has been verified by means of measurements. In **Figure 4** the Lissajous cycles measured for the humidity rates investigated are perfectly overlapped, therefore the average power supplied in the three cases is the same. A similar result has been obtained by using Power Supply 2.

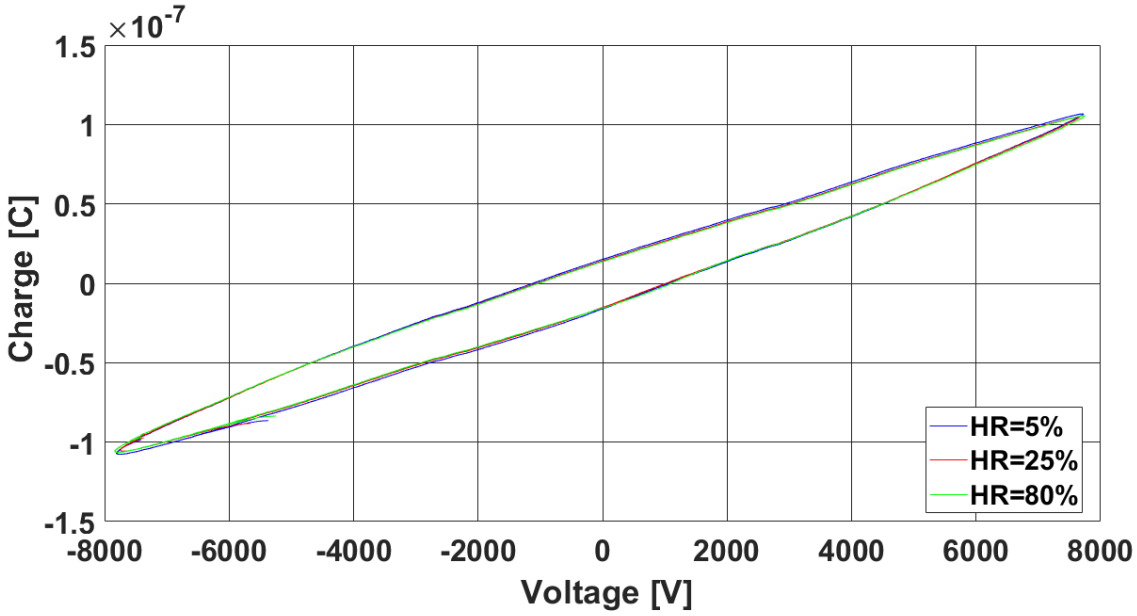

Figure 4. Lissajous figures obtained with the Power Supply 1 with 5 %, 25 % and 80 % humidity rate.

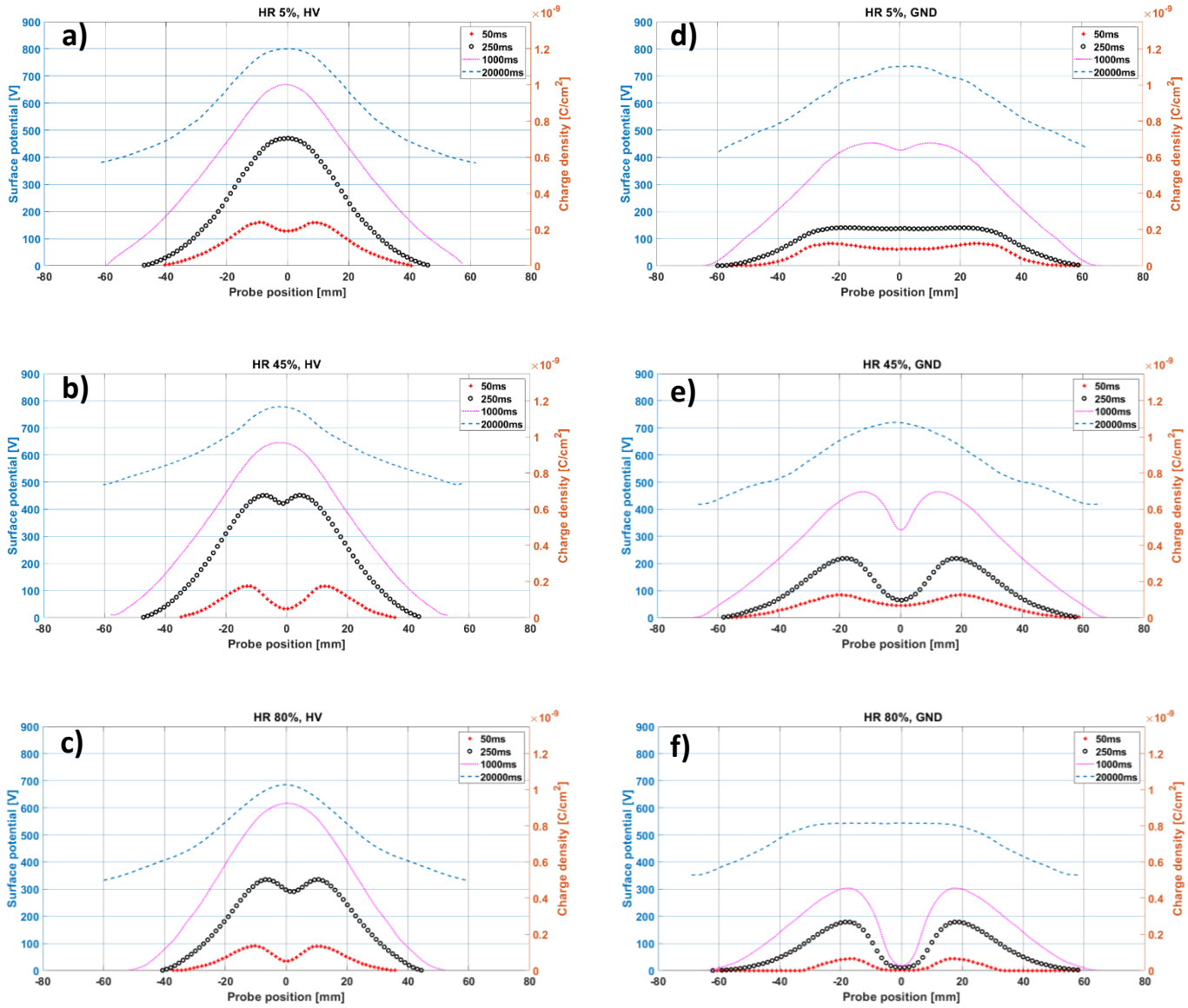

Figure 5. Surface potential distribution measured by increasing plasma-on time and under different humidity conditions (HR 5%, 45%, and 80%), with the Power Supply 1. The left-hand side graphs refer to the exposed electrode connected to the high voltage and the right-hand side to the exposed electrode when grounded.

In **Errore. L'origine riferimento non è stata trovata.**, the surface potential measured on the Plexiglass tray placed at a distance of 20 mm from the actuator surface, for different switching-on time intervals of the discharge and the three different humidity rates above mentioned (5 %, 45 %, and 80 %), are shown. Four switching-on time intervals have been investigated: 50 ms, 250 ms, 1 s, and 20 s. In the left-hand side of the figure, the exposed electrode has been connected to the high voltage terminal. In the right-hand side, it has been grounded. The zero 'probe position' refers to the centre of the jet, over the tray. In both graphs the charges deposited on the Plexiglass surface always induce a positive potential. This suggests that charges transported by the jet flow are positive ions. This is in agreement with the results presented in Ref. [26], in which we suppose that a possible candidate is the H3O+ ion. It is produced in relatively high amounts in air discharges even if the humidity degree is quite low. Moreover, this ion is quite stable even at atmospheric pressure. Other measurements are working in progress about this ionic species. In agreement with Ref. [26] the potential measured and, therefore, the amount of charges deposited on the surface increase when the plasma-on time interval increases. In all

considered cases, similar time behaviours have been observed. Two peaks were initially observed to form an M-shaped potential profile symmetric with respect to the zero position. This morphology is the result of the jet impinging the Plexiglass plate. In the subsequent phase of the discharge, the plasma jet causes a spread of the deposited charges on the plate with a bell-shaped profile. For low humidity levels, the discharge-on time interval needed to fill the inner space within the 'M' shaped distribution leading to the bell-shaped distribution, is shorter. When the HV electrode is exposed (left-hand side of **Figure 5**), for a humidity rate of 5 % the bell-shaped distribution was obtained after a plasma discharge of 250 ms. When the humidity level increases, the plasma kinetics within the jet varies, the charged particles density and their deposition velocity decrease. After 20 s, the maximum value of the deposited charges is quite similar for all humidity values. The potential measured at the zero-position has been of 800 V for a humidity rate of 5 % and 700 V, for a humidity rate of 80 %. Similar results have been obtained when the exposed electrode has been connected to the ground terminal. Main differences are related with the lower values of the potential reached at 20 s and the longer times needed to transform the M-shaped potential distribution into the bell-shaped one. This indicates that, when the exposed electrode is at high voltage, the jet propagates in a faster way with respect the one generated when the grounded electrode is exposed. Moreover the time needed for charged particles to be deposited on the target surface increases, as observed in Ref. [26] too. Therefore, the transition from M-shaped to bell-shaped distribution takes place in a longer time.

In all tests, for long plasma-on time intervals, the potential bell-shaped distribution is large with wings which do not reach the zero-value on the tray surface. The distributions reported in Ref. [26], obtained in open air, do not present this high value of the surface potential into the wings. The reason is the small dimensions of the box utilized in this work. Indeed, for long plasma ignition time intervals, the charged particles are transported and accumulated inside the Plexiglass tray. Therefore, the potential induced in the wings of the bell-shaped distribution increases with respect of that of Ref. [26] where the charges are driven forward further. In order to evaluate the rate with which charges are deposited on the target surface, the maximum value of the potential distribution as a function of the discharge on-time are shown in **Figure 6**. Results are shown when the exposed electrode has been at high voltage (**Figure 6 a**) and when grounded (**Figure 6 b**). For bell-shaped distributions, **Figure 6** displays maximum values of the measurements. In **Figure 6**, for M-shaped distributions, the average value between the maximum and the value measured at the centre of the M-shape are reported.

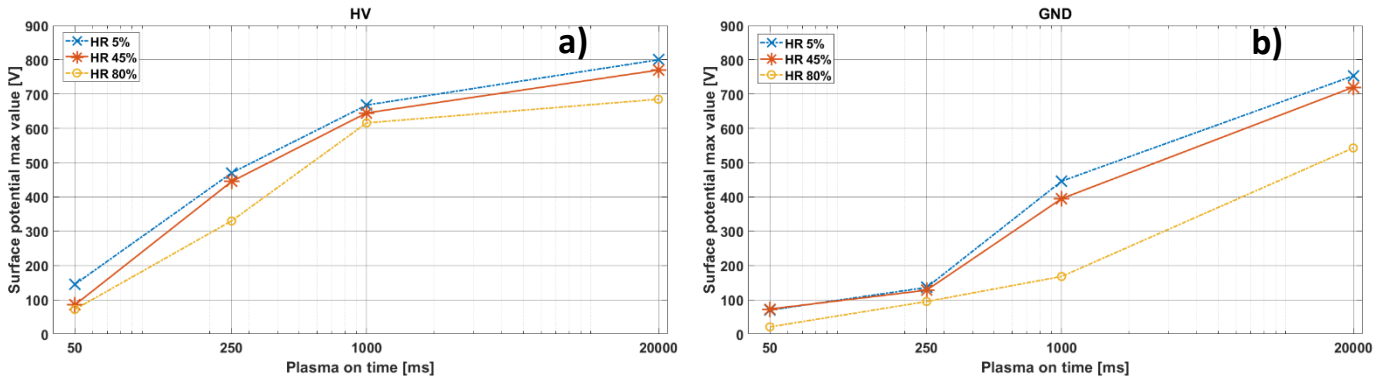

Figure 6. Surface potential maximum value as a function of the plasma on time, for different humidity levels. The left-hand side graphs refer to the exposed electrode connected to the high voltage and the right-hand side to the exposed electrode when grounded.

When the high voltage electrode is exposed, two-time behaviours are observed. Up to 1 s of the discharge-on time intervals the maximal value of the surface potential develops exponentially with the time interval. For longer time intervals a saturation occurs. For the highest humidity rate investigated (80%), induced potential values are about 50 % lower with respect the lowest humidity rate (5 %) for the discharge on-time of 50 ms. By increasing the plasma on-time, this difference decreases, reaching the value of 15 % after 20 s.

When the exposed electrode is grounded, a longer time is needed to start to deposit charges. Saturation effect is thus not clearly detectable for all time intervals considered.

For both configurations, the results obtained in ambient conditions (HR = 45 %) are very close to the measurements at low humidity conditions (HR = 5 %). At an HR of 5 % the highest amount of deposited charges on the target surface has been detected. The charge amount at 45 % HR is near this value. Therefore, the ambient condition (HR = 45 %) is already very close to the best working condition. Thus, a high number of free charges are deposited by the PSJA without the need of a controlled atmosphere. In fact, this indicates that this type of devices is suitable and effective for its utilization for real life treatment of surfaces for sterilization purposes.

In order to investigate the role of the electric field in the deposition of the charged particles, the electric field distribution induced on the actuator surface by the two utilized Power Supplies has been calculated. The electrostatic simulation has been carried out by using FEMM Software [32], avoiding the presence of both discharge and free charges. The input of the simulation is the voltage applied to the electrode. This value is set to 6 kV for Power Supply 1 and 12 kV for Power Supply 2. Electric field magnitude calculated on to the actuator surface is displayed in Figure 7.

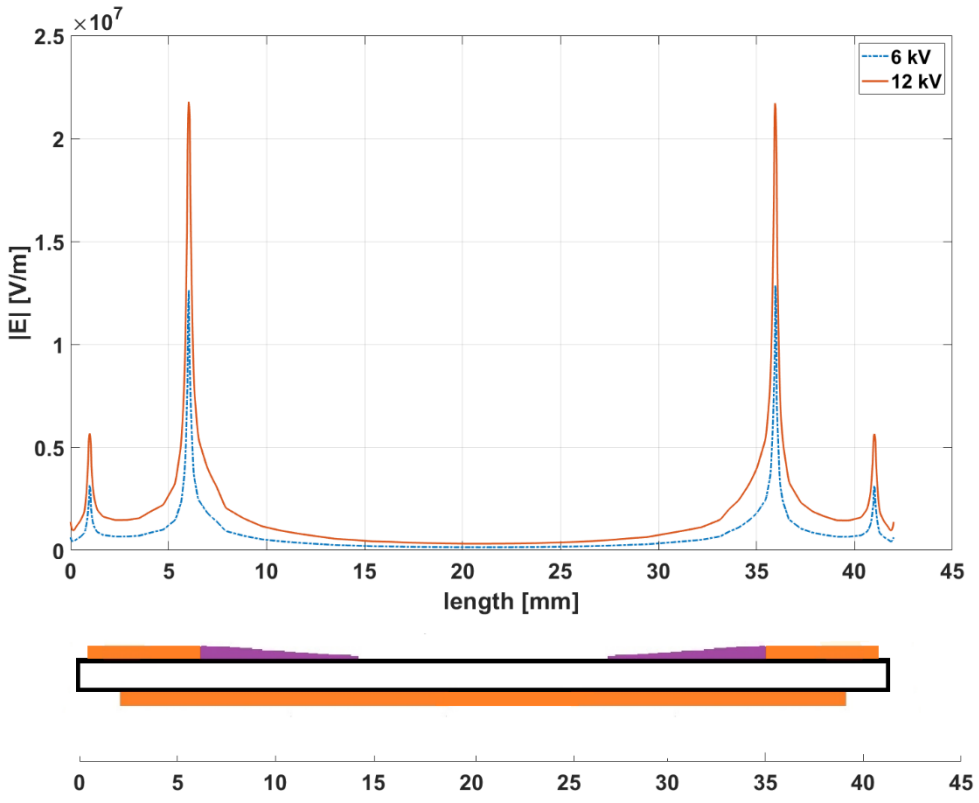

Figure 7. Electric field simulation results for the two power supplies.

The value of the electric field on the surface for the voltage of 12 kV is about twice of the one at obtained at a voltage of 6 kV.

In **Figure *8***, the surface potential distributions measured on the Plexiglass surface, as a function of the discharge-on time interval for Power Supply 2 are shown. The experimental set-up (except the power supply) and the experimental conditions has been the same used with the tests performed with Power Supply 1, the humidity rate of 45 % was utilized. These tests have been done with the exposed electrode connected to the high voltage terminal. For the discharge-on time of 20 s, the surface potential distribution reaches a value 15 % higher than the one obtained with Power Supply 1 (**Errore. L'origine riferimento non è stata trovata.** b). The bell-shaped distributions are broader than those measured at higher frequency and lower voltage. Already at 250 ms charges are attached onto side walls preventing the potential distribution wings to reach the zero value. Moreover, the surface potential distribution appears to be always bell-shaped even for the discharge-on time intervals tested. Even for a time interval of 50 ms it is nearly bell shaped. The results point out that a higher amount of charges transported by the flow is obtained when a higher electric filed is utilized (in this case 12 kV in place of 6 kV).

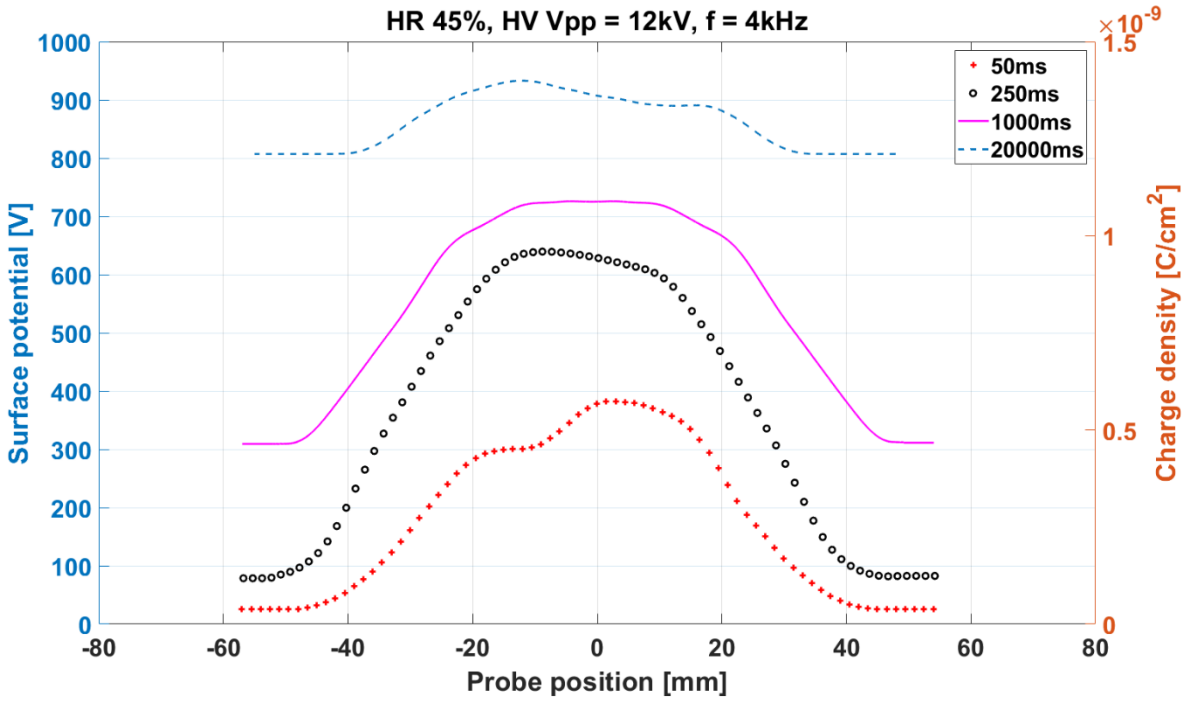

Figure 8. Surface potential distribution obtained with Power Supply 2 at a humidity rate of 45 % and for the four discharge-on time intervals.

A faster build-up mechanism is obtained when Power Supply 2 is utilized than that obtained with Power Supply 1, as shown in

Figure 9. Here the maximum surface potential values, obtained from the data reported in **Figure 8**, are displayed as a function of discharge-on time. In the figure, the data measured with Power Supply 2 are compared with those obtained by using Power Supply 1 in the same humidity rate conditions (see

Figure *6* a). When the transported charges hit the Plexiglass surface, when the surface is not charged (50 ms of plasma-on time), the potential maximum value induced by Power Supply 2 is about four times larger than the one obtained by

Power Supply 1. Therefore, the amount of charges deposited on the surface when Power Supply 2 is utilized, is about four times larger than that of Power Supply 1. In fact, as the discharge-on time increases, the electric potential induced by the charges already deposited on the surface prevent the fast increase of the charge deposition. Hence the difference of the surface potential values obtained by the two power supplies is reduced (see **Figure 9**). The considerable amount of charge deposition of Power Supply 2 in the first tens of milliseconds, limits a further significant increase of the surface deposition in front of the actuator. Incoming charges are driven forward and are accumulated on the lateral area of the surface and increase the surface potential of wings of the bell-shaped distribution. This behaviour is shown by the charge distribution of long discharge-on time intervals (20 s). When Power Supply 1 is used (Errore. L'origine riferimento non è stata trovata. **b**), charges are deposited in a bell-shaped distribution with decreasing wings. When Power Supply 2 is used, charge distribution is almost flat, indicating that a large number of charged particles reaches the box walls (**Figure 8**).

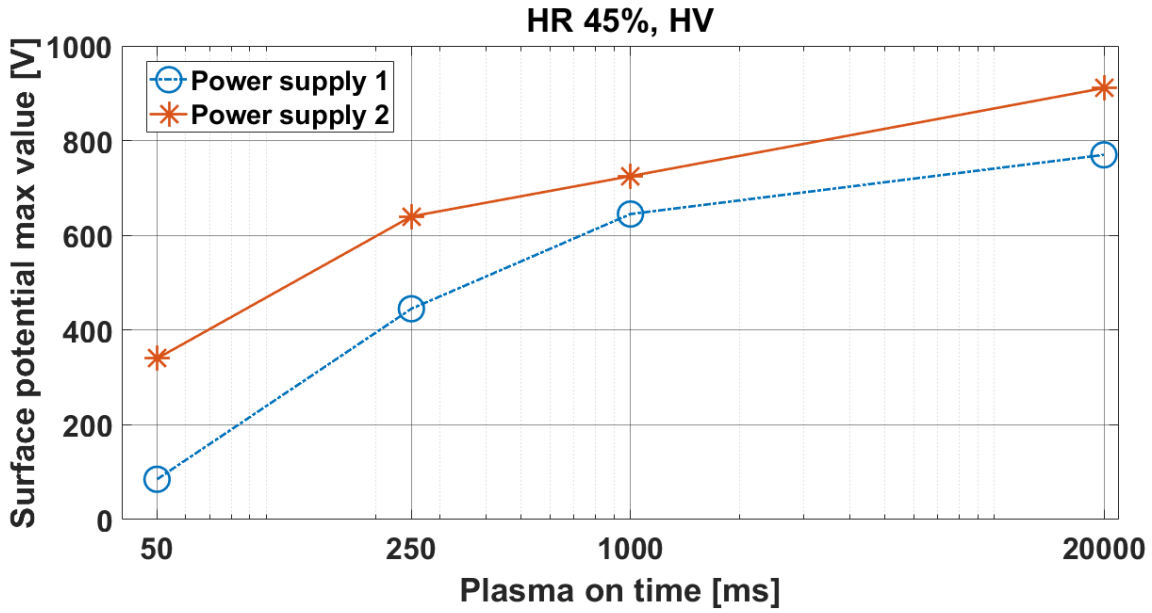

Figure 9. Surface potential values induced by the two power supply systems, as a function of plasma-on time.

4. Conclusions

The influence of air humidity and electric parameters on the discharge regime and the charged particles transported by the induced flow of a PSJA has been investigated.

The main result about humidity variation is that this parameter does not significantly influence the discharge regime. For the electric parameters utilized in this work, the average power feeding the discharge has been observed to be the same for all the humidity range investigated (humidity rate from 5% to 80 %). The charge build-up mechanism does not strongly depend on this parameter. The higher is the humidity, the higher is the time needed for transported charges to be deposited onto the target surface. The increase of the deposition time is increasing with the increase of the humidity rate investigated. The humidity, however, does not significantly affect the maximum value of deposited charges after a long discharge-on time. Therefore, this type of actuator can be utilized in ambient air without decreasing its biocidal effect. The use of ambient air as carrier gas, and the simple actuator set up make this device suitable for real-life large areas of indirect treatments for decontamination purposes.

When supplied with higher voltage and lower frequency, despite the same average power and EHD effects, the PSJA can deliver, toward a target, a higher amount of free charges. When the PSJA is supplied by 12 kV at 4.2 kHz, in the first tens of milliseconds, the number of charges deposited on the target is about four times than the one when the PSJA is supplied by 6 kV at 31 kHz. This could lead to an increase of biocidal effects of this device without increasing its power consumption, and thus, increasing both efficacy and efficiency.

References

[1] Fridman G, Friedman G, Gutsol A et al 2007 *Applied plasma medicine Plasma Process. Polym.* **5** 503–33

[2] Neretti G, Morandi B, Taglioli M, Poglayen G, Galuppi R, Tosi G and Borghi C A 2018 Inactivation of Eimeria oocysts in aqueous solution by a dielectric barrier discharge plasma in contact with liquid *J. Plasma Med.* **8** 155–62

[3] Neretti G, Ricchiuto A. C, Galuppi R, Poglayen G, Morandi B, Marotta E, Paradisi C, Tampieri F, Borghi C. A 2018 Indirect Inactivation of Candida guilliermondii by Using a Plasma Synthetic Jet Actuator: Effect of Advected Charged Particles. *Plasma Medicine.* **8** 255-268

[4] Pai K, Jacob J, 2013 Evaluation of dielectric barrier discharge configurations for biological decontamination. *51st AIAA Aerosp. Sci. Meet. Incl. New Horizons Forum Aerosp*. Expo. 1-15

[5] Song Y, Liu D, Lu Q, Xia Y, Zhou R, Yang D, Ji L, Wang W, 2015 An Atmospheric-Pressure Large-Area Diffuse Used for Disinfection Application. *IEEE Trans. Plasma Sci.* **43** 821-827.

[6] Xinyu L, Donghong L, Qisen X, Juhee A, Shiguo C, Xingqian Y, Tian D, 2016 Inactivation mechanisms of non-thermal plasma on microbes: A review. *Food control* **75** 83-91.

[7] Morent R, and De Geyter N, 2011 Inactivation of Bacteria by Non-Thermal Plasmas. *Biomedical Engineering - Frontiers and Challenges.*

[8] Rooth J.R. 2001 *Industrial Plasma Engineering: Volume 2: Applications to Nonthermal Plasma Processing*.

[9] Fridman G, Brooks A.D., Balasubramanian M., Fridman A., Gutsol A., Vasilets V. N., Ayan H., Friedman G. 2007 Comparison of direct and indirect effects of non-thermal atmospheric-pressure plasma on bacteria. *Plasma Process. Polym*. **4** 370–5

[10] Moreau E 2007 Airflow control by non-thermal plasma actuators. *J. Phys. D: Appl. Phys.* **40** 605–36

[11] Borghi C A, Carraro M R, Cristofolini A, and Neretti G 2008 Electrohydrodynamic interaction induced by a dielectric barrier discharge. *J. Appl. Phys.* **103** 063304

[12] Taglioli M, Shaw A, Wright A, FitzPatrick B, Neretti G, Seri P, Borghi C A and Iza F 2016 EHD-driven mass transport enhancement in surface dielectric barrier discharges. *Plasma Sources Science and Technology.* **25** 06LT01

[13] Benard, N., Caron, M., Moreau, E. 2017 Highly time-resolved investigation of the electric wind caused by surface DBD at various ac frequencies. *Journal of Electrostatics.* **88** 41-48

[14] Corke C, Post M L, Orlov D M. 2007 SDBD plasma enhanced aerodynamics: concepts, optimization and applications. *Prog. Aerosp. Sci*. **43** 193–217

[15] Dragonas F A, Neretti G, Sanjeevikumar P, Grandi G 2015 High-voltage high-frequency arbitrary waveform multilevel generator for DBD plasma actuators. *IEEE Trans. Ind. Appl.* **51(4)** 3334-3342

[16] Orlov D M, Font G I and Edelstein D 2008 Characterization of discharge modes of plasma actuators. *AIAA J*. **46(12)** 3142–8

[17] Alec W. Houpt, and Sergey B. Leonov 2017 Charge Transfer in Constricted Form of Surface Barrier Discharge at Atmospheric Pressure. *Journal of Thermophysics and Heat Transfer* **31(1)**

[18] Cristofolini A, Borghi C A, Neretti G. 2013 Charge distribution on the surface of a dielectric barrier discharge actuator for the fluid-dynamic control. *J. Appl. Phys.* **113** 143307

[19] D.HongaH., RabataY., K.Pub, A.Leroyc 2013 Measurement of the surface charging of a plasma actuator using surface DBD. *Journal of Electrostatics.* **71(3)** 547-550

[20] N.Takeuchia, T.Hamasakia, K.Yasuokaa, T.Sakuraib 2011 Surface charge measurement in surface dielectric barrier discharge by laser polarimetry. *Journal of Electrostatics.* **69(2)** 87-91

[21] Cristofolini A., Neretti G., Borghi C.A. 2013 Effect of the charge surface distribution on the flow field induced by a dielectric barrier discharge actuator. *J. Appl. Phys.* **114** 073303

[22] Neretti G, Seri P, Taglioli M, Shaw A, Iza F and Borghi C A 2017 Geometry optimization of linear and annular plasma synthetic jet actuators. J. Phys. D: Appl. Phys. **50** 015210

[23] Santhanakrishnan A and Jamey D J 2007 Flow control wit plasma synthetic jet actuators. *J. Phys. D: Appl. Phys.* **40** 637

[24] Fridman A, Kennedy L A, 2004 Plasma Physics and Engineering (Boca Raton, FL: CRC Press)

[25] Fridman A, Chirokov A, and Gutsol A. 2005 Non-thermal atmospheric pressure discharges. *J. Phys. D: Appl. Phys*. **38** R1–R24

[26] Neretti G, Ricchiuto A C and Borghi C A 2018 Measurement of the charge distribution deposited by an annular plasma synthetic jet actuator over a target surface. *J. Phys. D: Appl. Phys.* **51** 324004

[27] Abdelaziz A A, Tatsuo I and Takafumi S 2018 Humidity effects on surface dielectric barrier discharge for gaseous naphthalene decomposition. *Physics of Plasmas*. **25** 043512

[28] Neretti G, Cristofolini A and Borghi C A. 2014 Experimental investigation on a vectorized aerodynamic dielectric barrier discharge plasma actuator array. *J. Appl. Phys*. **115** 163304

[29] Neretti G, Ricco M 2019 Self-Tuning High-Voltage and High-Frequency Sinusoidal Power Supply for Dielectric Barrier Discharge Plasma Generation. *Electronics.* **8** 1137

[30] Neretti G, Cristofolini A., Borghi C.A., Gurioli A., Pertile R. 2012 Experimental results in DBD plasma actuators for air flow control. *IEEE Trans. Plasma Sci.* **40(6)** 1678–87

[31] Pon J, Moreau E and Touchard G 2005 Assymmetric surface dielectric barrier discharge in air at atmospheric pressure: electrical properties and induced airflow characteristics. *J. Phys. D: Appl. Phys.* **38** 3635–42

[32] Meeker D C, *Finite Element Method Magnetics*, Version 4.2, http://femm.info